Defence Science Journal, Vol. 57, No. 3, May 2007, pp. 233-239

Modified Lead-zirconate-titanate for Pyroelectric Sensors

O.P. Thakur[1], J.P. Singh[1], Chandra Prakash[2], and Pran Kishan[3]

[1]*Solid State Physics Laboratory, Delhi-110 054*
[2]*Directorate of ER&IPR, DRDO Bhawan, New Delhi-110 011*
[3]*Institute of Defence Scientists & Technologists, C/o CFEES, Delhi-110 054*

ABSTRACT

Pyroelectric sensors based on ceramic materials have found applications in IR detection in defence and civil systems. To develop suitable ceramic material for IR detector applications, a modified PZT system with compositional formula $Pb_{1-x}Sm_x(Zr_{0.58}Fe_{0.18}Mn_{0.02}Nb_{0.2}Ti_{0.02})O_3$ where $0 \le x \le 0.025$ was synthesised by conventional solid state reaction method. The materials were characterised for their properties like dielectric and pyroelectric coefficient. Hysteresis loop was recorded at room temperature. The sample with 2 mole per cent samarium (*Sm*) substitutions was found to be more promising for sensor application based on its high material's figure of merit (FOM). Sensors fabricated with this material were integrated with FET amplifier. The devices configured with compensating element were evaluated for different chopping frequencies. The value of material's FOM, F_D, and detectivity, D^*, were determined from measured parameters and were, 3.6×10^{-5} $Pa^{-1/2}$ and 2×10^8 $cmHz^{1/2}/W$, respectively.

Keywords: PZT, pyroelectric sensors, ceramic materials, sensors, IR detectors, lead-zirconate-titanate systems

1. INTRODUCTION

A pyroelectric sensor is made of ceramic material that generates a surface charge when exposed to IR radiation[1-3]. As the amount of radiation changes, so does the charge. Being a high impedance signal, a field effect transistor (FET) is used to buffer this potential as shown in Fig. 1. This sensor is sensitive to a wide range of radiation. To optimise for detection, a filter window is added to limit the incoming radiation to desired wavelength range of 8 µm to 14 µm. It is shown in Fig. 2 with an external resistor to convert the FET current to a voltage.

The output voltage is a function of the amount of infrared (IR) radiation sensed at the input. Unfortunately, the output is also affected by vibration, radio interferences, and sunlight. Figure 3 shows an improved sensor with dual elements. The sensing element is connected such that one subtracts from the other. This arrangement causes any signal common to both elements to be cancelled out. An object to

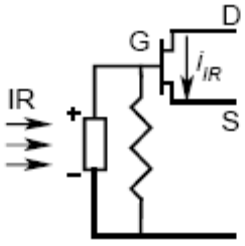

Figure 1. Pyroelectric charge measured with a field effect transistor.

Revised 29 November 2006

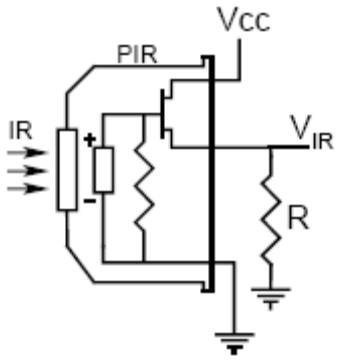

Figure 2. Single-element pyroelectric detector.

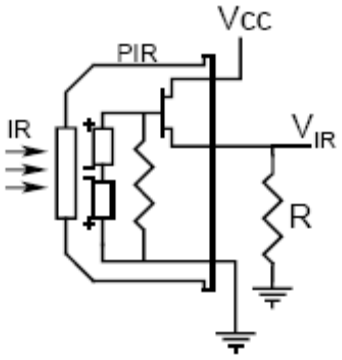

Figure 3. Dual-element pyroelectric detector.

be detected in front of the sensor activates main element while vibrations, and other background signals, affect both elements simultaneously and are cancelled out[4].

The pyroelectric effect can be observed only in those materials whose point group symmetry is consistent with the vectorial property of the polarisation. Thus, crystalline materials whose structures belong to the ten polar point groups namely: l, *m*, 2, *mm*2, 3, 3*m*, 4, 4*mm*, 6, 6*mm* and ceramics, polymeric and composite materials whose structures belong to the textural or basic Curie point groups (∞, ∞m) are pyroelectric materials. Thus, the pyroelectrics can be classified into two main categories: (i) non-ferroelectric pyroelectrics are those whose polarisation cannot be switched by an application of external electric field (including some semiconductors and biological materials), and (ii) ferroelectric pyroelectrics are those whose polarisation is obtained by poling and also can be switched by an electric field. The pyroelectric effect of ferroelectric pyroelectrics usually exists below a certain transition temperature called the Curie point, T_c, in the proper ferroelectrics and is more temperature dependent than that of the non-ferroelectric pyroelectrics[5].

To find out suitable material for any particular application, material's figure of merit (F_D) and voltage responsivity (R_v) should be known. For a given detector area and thermal time constant, (F_D) and F_v are given by

$$F_D = p'/c' \ (\varepsilon\varepsilon_o \tan\delta)^{1/2}$$

and $F_v = p'/c' \ \varepsilon\varepsilon_o$

where p' is the pyroelectric coefficient, c' is the volume specific heat, ε is the dielectric constant and $\tan\delta$ is the loss tangent. For detector performance detectivity, D^*, (which relates to the material's F_D) and voltage responsivity are studied.

Pyroelctric IR detectors can be used at room temperature and these can be used to detect radiation in the full range of electromagnetic spectrum. Ferroelectric ceramics based on titanate, zirconate and niobate oxides exhibit high permittivity and are widely used for diverse applications as vidicon targets, IR detectors, medical imaging, etc[6].

Ceramics based on lead-zirconate-titanate (PZT) are now widely used in various pyroelectric devices, as are tryglycine sulphate and lithium tantalate single crystals[7,8]. Among the distinctive features of PZT are high sensitivity, non-hygroscopicity, mechanical strength, simplicity of preparation and poling in a given direction. The main advantage of the $Pb(Zr,Ti)O_3$ series is the possibility of controlling their electro-physical properties and Curie temperatures using modifying additions.

There are reports available on the substitution of *Sr*, *Ca* in modified PZT system[9,10,] but there is no report available of the rare earth substitution in the present system. Therefore in the present work, the dielectric and pyroelectric properties of modified PZT ceramics with *Sm* substitution at *Pb*-site (A-site) have been studied and the response of detector in terms of its responsivity and detectivity have also been investigated.

2. EXPERIMENTAL PROCEDURE

Polycrystalline samples of composition $Pb_{1-x}Sm_x(Zr_{0.58}Fe_{0.18}Mn_{0.02}Nb_{0.2}Ti_{0.02})O_3$ were prepared from high purity PbO, Sm_2O_3, ZrO_2, Fe_2O_3, MnO_2, Nb_2O_5 and TiO_2 using high-temperature solid-state reaction technique. These ingredients taken in stoichiometry were mixed thoroughly in Ball-mill using zirconia balls as grinding medium in liquid medium and dried by slow-evaporation for 12 h in an oven. The dried powders of the compounds were then calcined twice followed by milling and drying at 800 °C and 850 °C for 4 h respectively. The processes of mixing and calcination were repeated twice to get the homogeneous powders. Compaction of powder in rod form was done using cold isostatic press by applying pressure ~150 MPa. These rods were then sintered at 1250 °C for 3h to obtain high density (~96 % of the theoretical value) in a sealed alumina crucible under a lead-rich atmosphere. Rectangular slices (5.5 x 4 x 0.2 mm) were cut out of the sintered rod. The quality and formation of the compounds were checked using x-ray diffraction technique at room temperature using Philips powder diffractometer with $CuK\alpha$ radiation (λ = 0.15418 nm) in a wide range of 2θ ($20^o \leq 2\theta \leq 80^o$) at a scanning rate of 2 °/min. For electrical characterisation, both the major phases of rectangular slices were electroded with sputtered gold. Measurements of capacitance and dissipation factor were carried out by HP 4284A LCR meter interfaced with PC, both as a function of frequency (100 Hz-1MHz) and temperature (30 °C–250 °C) in heating mode (1 °C/min). From the capacitance measurements, the dielectric permittivity was determined whereas the dissipation factor was used to calculate the tangent loss at different frequencies and temperatures.

Polarisation switching was observed using a Sawyer-Tower circuit at 50 Hz. Samples were immersed in a silicone oil to prevent electrical breakdown of the specimen. Patterned slices were poled at 175 °C for 30 min with applied dc field of 20 kV/cm. Samples were kept short circuited overnight to neutralise the surface charge accumulated during poling. Pyro current was measured by heating the test sample at fixed heating rate and measuring the current using Keithley Electrometer Model 6517. The pyro coefficient was calculated using the formula $p'=i/A$(heating rate), where p' is the pyroelectric coefficient; i is the current, and A is the area of the sample[11,12].

3. RESULTS AND DISCUSSION

The typical x-ray diffraction pattern for the nominal composition with x = 0.02 is shown in Fig. 4. The sharp and single XRD peaks of all the samples suggest the formation of single-phase compounds with rhombohedral structure.

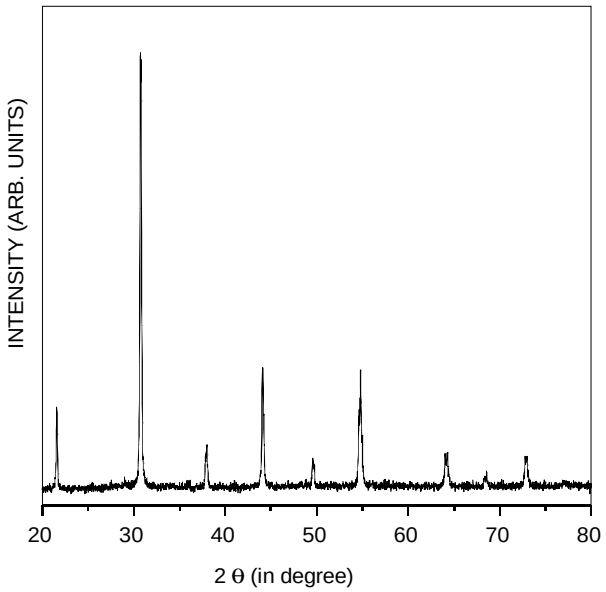

Figure 4. Typical XRD pattern of the optimised composition (x = 0.02).

Table 1 lists the dielectric constant, dielectric loss (measured at 1 kHz) and the transition temperature, T_c (as determined from ε' *vs* T plots) for all the compositions. It is evident that the value of dielectric constant increases while dielectric loss decreases with *Sm* concentration. The transition temperature decreases with *Sm* concentration as shown in Table 1. Although the pyroelectric coefficient continues to increase with increase in *Sm* level, the figure of merit is maximum for x = 0.02 sample; since F_D is proportional to $(\varepsilon' \tan\delta)^{-1/2}$. Figure 5 illustrates the temperature-dependence of dielectric behaviour for optimised composition, x = 0.02. It follows the typical characteristics of ferroelectric

Table 1. Dielectric, pyroelectric properties and material's figure of merit of $Pb_{1-x}Sm_x(Zr_{0.58}Fe_{0.18}Mn_{0.02}Nb_{0.2}Ti_{0.02})O_3$ system.

x	ε' at 1 kHz	tan δ at 1 kHz	T_c (°C)	p' (10^{-4}C/m^{2}K)	F_D (10^{-5}Pa$^{-1/2}$)
0.000	410	0.070	217	5.00	1.30
0.005	415	0.025	206	5.10	1.35
0.010	425	0.015	198	5.30	2.00
0.015	435	0.012	186	5.50	2.50
0.020	460	0.008	176	5.75	3.60
0.025	750	0.013	152	6.30	2.40

materials and passes through maxima at 176 °C, the value of dielectric constant (ε') and loss tangent (tan δ) decreases with higher frequencies. The variation of dielectric constant is almost invariant up to 100 °C, which is desirable for sensor application to get stable response.

The frequency-dependency of dielectric behaviour is shown in Fig. 6 at two different temperatures over the frequency span of 100 Hz-1 MHz. The dielectric constant remains almost invariant with frequency while dielectric loss shows little variance at lower frequency region. The value of dielectric constant and loss is obviously high at higher temperature as it is approaching towards transition temperature. The DC resistivity of the material is high (~1010 ohm-cm) which helps in eliminating the gate bias resistance from the detector assembly.

The typical hysteresis loop for the composition with x = 0.02 is shown in Fig. 7 which shows well-saturated loop. The value of remanent polarisation

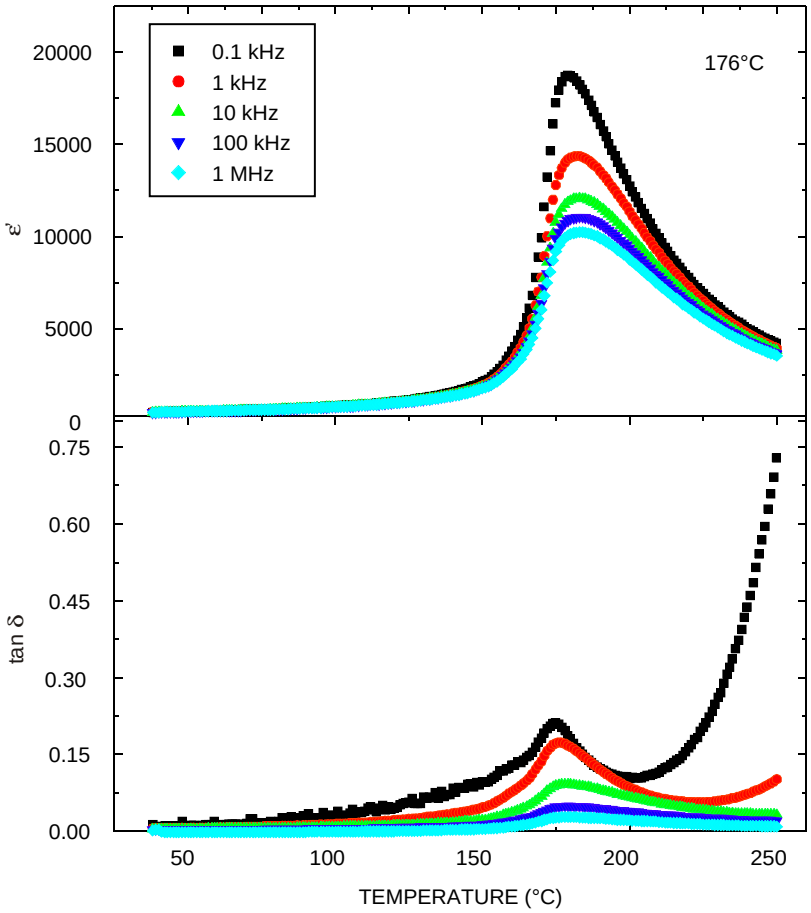

Figure 5. Temperature dependence of ε' and tan δ at different frequencies for x = 0.02.

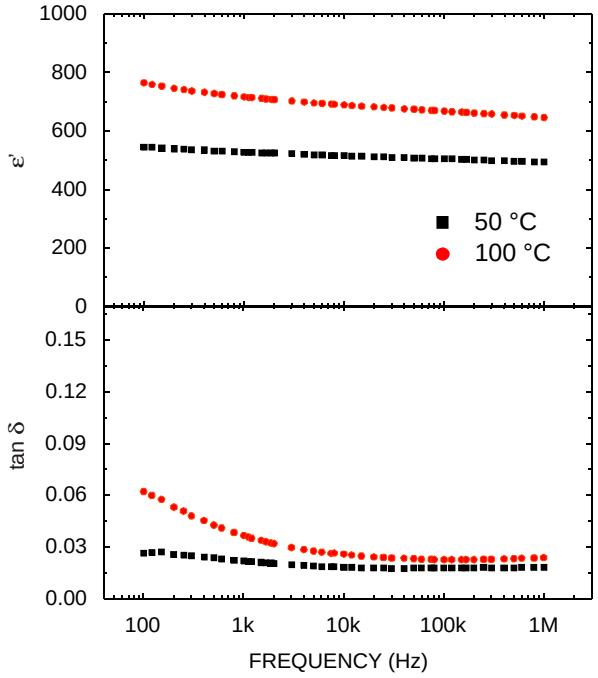

Figure 6. Frequency dependence of ε' and tan δ at different frequencies for x = 0.02.

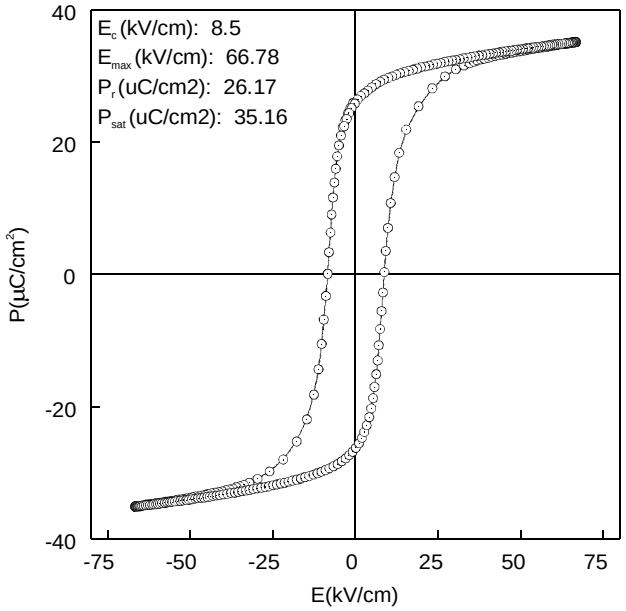

Figure 7. Typical hysteresis loop for the composition with *Sm*, x = 0.02.

(P_r), saturation polarisation (P_{sat}), coercive field (E_c) and maximum electric field (E_{max}) is shown as an insert in Fig. 7.

The detectivity of pyro elements was characterised using typical arrangement as shown in Fig. 8.

Sensor was tested with a black body temperature of 500 K and at an incident energy of 75 μW/cm^2 falling on the sample. A chopped beam of radiation is incident upon the front electrode. For the chopping period less than the thermal time constant of the sample, Shaulov[13], *et al*. have shown that in steady state, mean temperature of the sample rises linearly when a radiation pulse is incident on the sample and falls linearly between pulses. In the present test set up, the chopping period was kept much less than electrical time constant, thereby obtaining a triangular voltage response. The specific detectivity and responsivity are shown in Figs 9 and 10 respectively. Both of the plots show maxima in the range of 3-6 Hz. The broad range of maxima depends upon the thermal and electrical time constant of sensor element. The usable range of maxima for this parameters depend upon the applications, and thereby

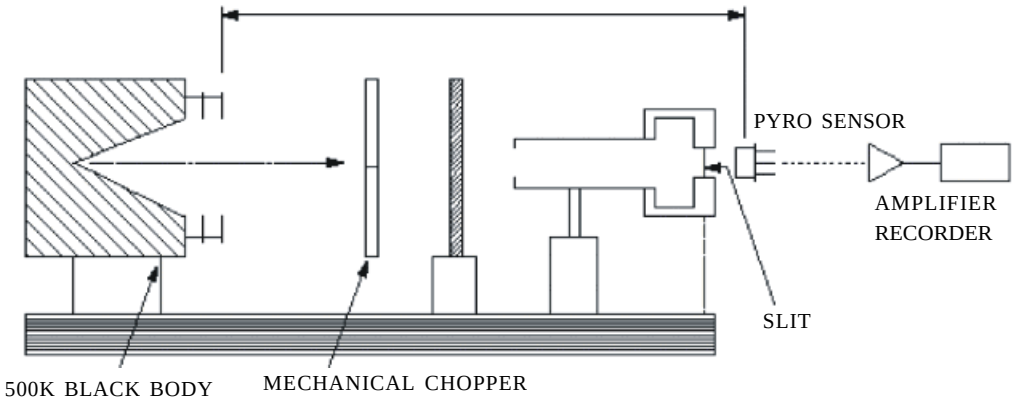

Figure 8. Experimental setup for detectivity and responsivity measurement of the pyro sensors.

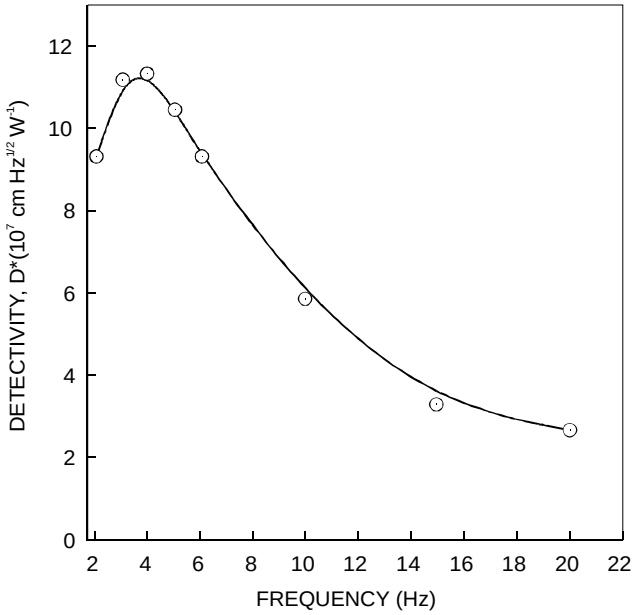

Figure 9. Frequency dependence of specific detectivity for the composition with x = 0.02.

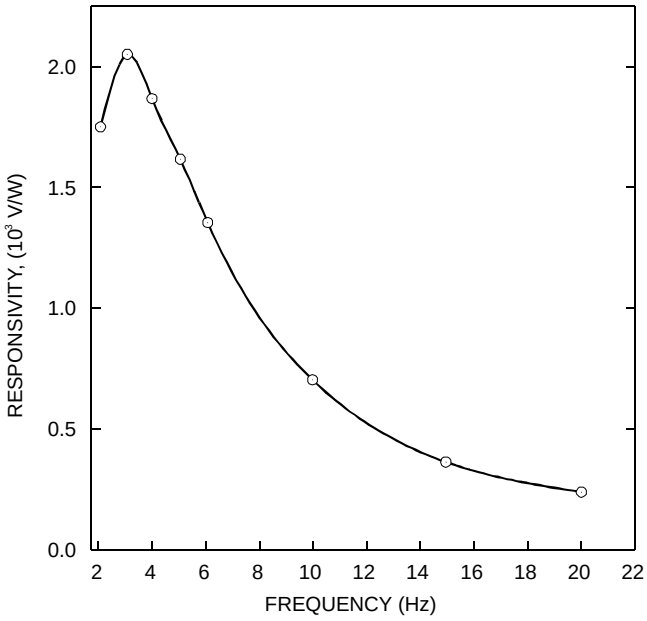

Figure 10. Frequency dependence of voltage responsivity for the composition with x = 0.02.

can be adjusted to desired range by tailoring the value of resistance and capacitance of sensor element and resistance of amplifier circuit[14].

4. CONCLUSIONS

The composition with x = 0.02 was found to give the highest value of pyroelectric F_D. The pyroelectric F_D of this composition are comparable with that of other widely used ceramics. The dc resistivity of the material is high which renders in eliminating the gate bias resistance from the amplifier circuit of the detector. So, it can be concluded that $Pb_{1-x}Sm_x(Zr_{0.58}Fe_{0.18}Mn_{0.02}Nb_{0.2}Ti_{0.02})O_3$ composition with x = 0.02 is a suitable material for IR detectors.

REFERENCES

1. Watton, R. Ferroelectric materials and devices in infra detection and imaging. *Ferroelectrics*, 1989, **91**, 87-108.

2. Guggilla, P.; Batra, A.K.; Curry, J.R.; Aggarwal, M.D.; Alim, M.A. & Lal, R.B. Pyroelectric ceramics for infrared detection applications. *Materials Letters*, 2006, **60**, 1937.

3. Guggilla, P.; Batra, A.K.; Aggarwal, M.D. & Lal, R.B. Investigation on nanocomposites for pyroelectric infrared sensors. *Proceedings SPIE*, 2005, **5725**, 295.

4. Whatmore, R.W. Pyroelectric devices and material. *Rep. Prog. Physics*, 1986, **49**, 1335-386

5. Luff, D.; Lane, R.; Brown, K.R. & Marshallsay, H.J. Ferroelectric ceramics with high pyroelectric properties. *J. Brit. Ceramic Soc.*, 1974, **73**, 251-64.

6. Moulson, A.J. & Herbert, J.M. Electroceramics: Materials, properties and applications. Chapman and Hall, London, 1990.

7. Porter, S.G. Materials for pyroelectric detectors. *Materials and Design*, 1987, **8**, 120.

8. Burgess, D.E. Infrared detectors and arrays. *SPIE Proceedings*, 1988, **930**, 139.

9. Osbond, P.C. & Whatmore, R.W. Improvements to pyroelectric ceramics via strontium doping of the lead zirconate-lead iron niobate-lead titanate system. *Ferroelectrics*, 1991, **118**, 93-101.

10. Whatmore, R.W. Pyroelectric ceramics and devices for thermal infra-red detection and imaging. *Ferroelectrics*, 1991, **118**, 241-59.

11. Glass, A. Pyroelectric coefficient direct method technique and application to a nsec response time detector. *J. Appl. Phys.*, 1969, **40**, 4699.

12. Byer, R.L. & Roundy, C.B. *Ferroelectrics*, 1972, **3**, 333-38.

13. Shaulov, A. Direct measurement of pyroelectric figure of merit of proper and improper ferroelectrics. *J. Appl. Phys.*, 1979, **50**, 4913-919.

14. Putley, E.H. A method for evaluating the performance of pyroelectric detectors. *Infrared Physics*, **20**, 139-47